nature biomedical engineering

ARTICLES

https://doi.org/10.1038/s41551-019-0442-z

Use of a supramolecular polymeric hydrogel as an effective post-operative pericardial adhesion barrier

Lyndsay M. Stapleton[1,2], Amanda N. Steele[1,2], Hanjay Wang[2], Hector Lopez Hernandez[3], Anthony C. Yu[3], Michael J. Paulsen[2], Anton A. A. Smith[3], Gillie A. Roth[1], Akshara D. Thakore[2], Haley J. Lucian[2], Kailey P. Totherow[1], Sam W. Baker[4], Yuko Tada[5], Justin M. Farry[2], Anahita Eskandari[2], Camille E. Hironaka[2], Kevin J. Jaatinen[2], Kiah M. Williams[2], Hunter Bergamasco[2], Clifton Marschel[2], Blaine Chadwick[2], Frederick Grady[2], Michael Ma[2], Eric A. Appel[1,3]* and Y. Joseph Woo[1,2]*

Post-operative adhesions form as a result of normal wound healing processes following any type of surgery. In cardiac surgery, pericardial adhesions are particularly problematic during reoperations, as surgeons must release the adhesions from the surface of the heart before the intended procedure can begin, thereby substantially lengthening operation times and introducing risks of haemorrhage and injury to the heart and lungs during sternal re-entry and cardiac dissection. Here we show that a dynamically crosslinked supramolecular polymer–nanoparticle hydrogel, with viscoelastic and flow properties that enable spraying onto tissue as well as robust tissue adherence and local retention in vivo for two weeks, reduces the formation of pericardial adhesions. In a rat model of severe pericardial adhesions, the hydrogel markedly reduced the severity of the adhesions, whereas commercial adhesion barriers (including Seprafilm and Interceed) did not. The hydrogels also reduced the severity of cardiac adhesions (relative to untreated animals) in a clinically relevant cardiopulmonary-bypass model in sheep. This viscoelastic supramolecular polymeric hydrogel represents a promising clinical solution for the prevention of post-operative pericardial adhesions.

Adhesions are fibrous bands of scar tissue that form between internal organs and their surrounding tissues as a result of natural healing processes following surgery, bodily injury or inflammation. More than 20 million Americans undergo invasive surgery each year, and adhesions develop after 95% of all operations, regardless of the procedure or location in the body[1]. Following abdominal surgery, many patients experience post-operative adhesion-related complications such as severe pain and/or organ dysfunction, with 15–30% requiring a second operation to release the adhesions (that is, adhesiolysis)[2–6]. In cardiothoracic surgery, 6–17% of all coronary bypass and valve repair or replacement surgeries are reoperations[7–9], in which the presence of adhesions substantially lengthens operation times and magnifies the risk of injury to the heart, lung and great vessels during sternal re-entry and cardiac dissection. Patients with congenital heart disease, who represent nearly 1% of all live births[10], commonly require several redo cardiac operations over the course of a lifetime, such that 33% of all paediatric and congenital heart surgeries are reoperations[11]. Overall, the treatment of post-operative adhesions costs the United States healthcare system over US$2.5 billion annually, and adhesion-related complications result in nearly 1 million additional days of inpatient care each year, thus presenting a major unmet clinical need for effective post-operative adhesion barriers[12].

Current options for adhesion prevention consist of solid polymer or hydrogel films made from polysaccharides and/or synthetic polymers (resorbable and non-resorbable varieties) that are designed to serve as a physical barrier between scarring tissue and surrounding organs. The two most common commercial products are indicated for use only in the abdomen and are solid, resorbable membranes composed of hyaluronic acid and carboxymethylcellulose in the form of a film (Seprafilm, Sanofi/Genzyme) or a woven fabric (Interceed, Ethicon). In practice, these products are difficult to deploy to completely cover the target tissues and form an effective physical barrier. These barriers often fail to prevent or limit adhesions as they often degrade too quickly after surgery or become dislodged owing to natural tissue movement[13]. Furthermore, films and fabrics cannot be made to cover the entire surface area of tissues with irregular surfaces or those that are heavily folded (for example, great vessels of the heart and small intestine, respectively)[14]. Therefore, any uncovered intervening spaces remain at risk of adhesion formation despite the use of these sheet-like barriers.

To circumvent the difficulties associated with the application of solid barriers, sprayable polymer solutions comprising chitosan, hyaluronic acid and/or carboxymethylcellulose have been investigated[15–17]. While sprayable polymer solutions are simple to apply, they are only mildly effective at preventing adhesions because of their short residence time at the site of the injured or inflamed tissues[18,19]. Sprayable pre-polymer solutions that undergo in situ polymerization (for example, thiol-maleimide or thiol-acrylate Michael-addition reactions, amine-aldehyde or oxide-aldehyde imine-forming reactions, or photo-initiated radical polymerization) to form covalent hydrogels with tunable mechanical properties,

[1]Department of Bioengineering, Stanford University, Stanford, CA, USA. [2]Department of Cardiothoracic Surgery, Stanford University, Stanford, CA, USA. [3]Department of Materials Science & Engineering, Stanford University, Stanford, CA, USA. [4]Department of Comparative Medicine, Stanford University, Stanford, CA, USA. [5]Department of Cardiovascular Medicine, Stanford University, Stanford, CA, USA. *e-mail: eappel@stanford.edu; joswoo@stanford.edu

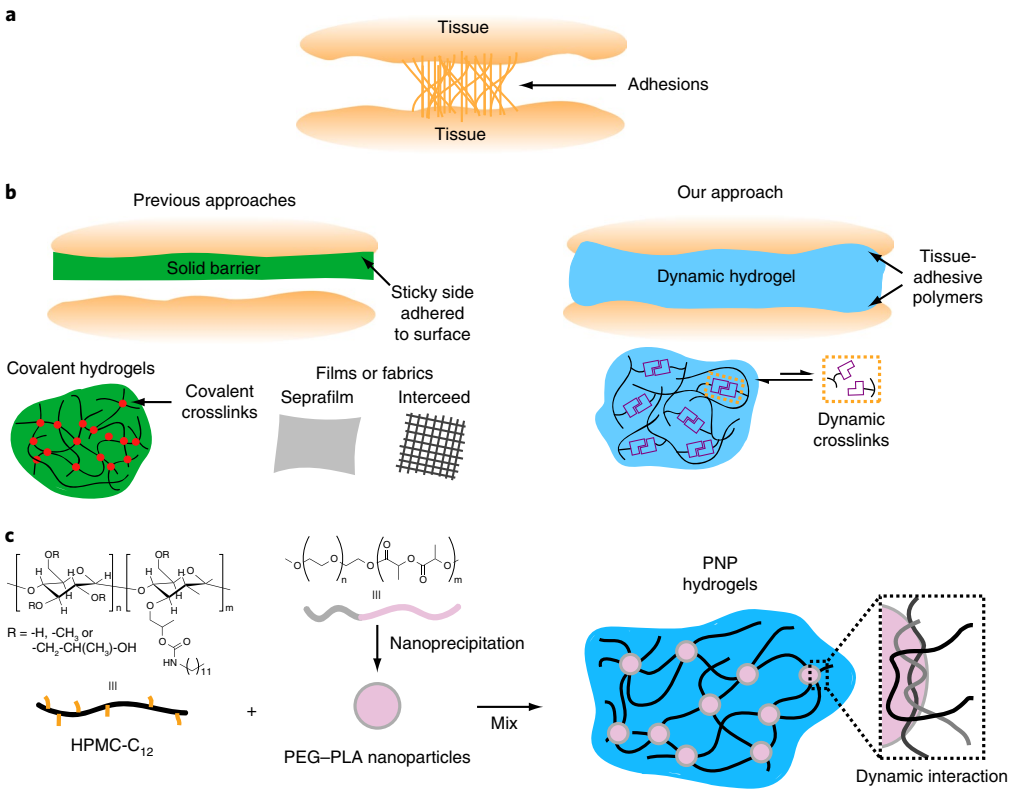

Fig. 1 | Overview of PNP hydrogel adhesion barrier. a, Schematic representation of adhesion formation between two tissues. **b**, Schematic representation of previous approaches to prevent adhesions using solid adhesion barriers to physically separate organs and tissues. Such stationary adhesion barriers include the two best-known commercial products, Seprafilm (film) and Interceed (fabric), and covalently crosslinked hydrogels formed by in situ polymerization of precursor macromers. Our approach uses dynamically crosslinked, shear-thinning, self-healing and viscoelastic polymer hydrogels that are placed between organs and tissues, allowing these structures to move naturally. **c**, Our materials exploit multivalent and dynamic non-covalent interactions between hydrophobically modified HPMC-C_{12} and PEG–PLA to form hydrogels that can be sprayed with standard equipment, adhere to tissue (HPMC-C_{12} is tissue adhesive) and provide a viscoelastic barrier between organs and tissues to inhibit adhesion formation.

similar to those of soft biological tissues, have been shown to increase the local residence time in the body[20–26]. However, the irreversibility of the crosslinks in these systems generally makes them brittle and/or unable to accommodate the dynamic movement of tissues in the body. These covalent hydrogel systems fracture and/or become dislodged, resulting in failure to inhibit adhesion formation[27]. Other potential side effects of in situ polymerization include crosslinking of the native tissues and greater adhesion formation due to the non-bioorthogonal nature of the chemistries used for hydrogel crosslinking[27]. Furthermore, marked swelling of these materials, reaching volumetric expansion in excess of 400%, can result in cardiac tamponade or mechanical compression of the heart[28,29]. Despite the overwhelming clinical need for adhesion barriers for abdominal and cardiothoracic surgery, commercial adhesion barriers have been poorly adopted in practice, with an application rate of less than 10% in candidate abdominal surgeries[30].

On the basis of these limitations, the ideal adhesion barrier should exhibit the following properties: (1) tunable shear-thinning and rapid self-healing to enable spraying or spreading on the tissue of interest; (2) tissue adherence to ensure local retention over clinically relevant time frames; (3) a high degree of biocompatibility; and (4) viscoelasticity, to enable organs and tissues to move freely relative to one another to effectively prevent adhesions (Fig. 1). Encompassing these characteristics, supramolecular polymeric hydrogels constitute a distinct alternative approach for post-operative adhesion prevention (Fig. 1b). These materials exhibit highly tunable viscoelastic mechanical properties, shear-thinning and rapid self-healing, which together enable them to be deployed by simple spraying or spreading using standard equipment, or by catheter delivery or direct injection[31–36]. Further, these types of materials do not appreciably swell like most covalently crosslinked hydrogels, because they typically dissolve as their dynamic crosslinks dissociate[32] (Supplementary Fig. 1). We previously developed a supramolecular polymeric hydrogel that exploits polymer–nanoparticle (PNP) interactions between hydrophobically modified cellulose derivatives and nanoparticles[32–34,37–42]. These PNP hydrogels are formed by simple mixing of aqueous solutions of dodecyl (C_{12})-modified hydroxypropylmethylcellulose (HPMC) (that is, HPMC-C_{12}) with biodegradable polymeric nanoparticles comprising poly(ethylene glycol)-b-poly(lactic acid) (PEG–PLA; b denotes the block copolymer) (Fig. 1c). In addition, the simplicity of their preparation through a self-assembly process enables PNP hydrogel manufacturing to be easily scaled up, producing materials with identical mechanical properties on any scale[43]. On the basis of the broadly tunable viscoelastic mechanical properties and excellent biocompatibility of PNP hydrogels[34], we hypothesized that this material could constitute a simple-to-deploy adhesion barrier to effectively prevent post-operative adhesions.

Viscoelastic and flow properties of the PNP hydrogel

Each of the suggested physical parameters describing the ideal adhesion barrier was modulated by alteration of the PNP hydrogel formulation. A series of PNP hydrogels comprising HPMC-C_{12} and PEG–PLA nanoparticles was created by controlling the concentration of both components; we denote hydrogel formulations as polymer:NP (wt%:wt%). PNP 1:10 and PNP 2:10 hydrogels both

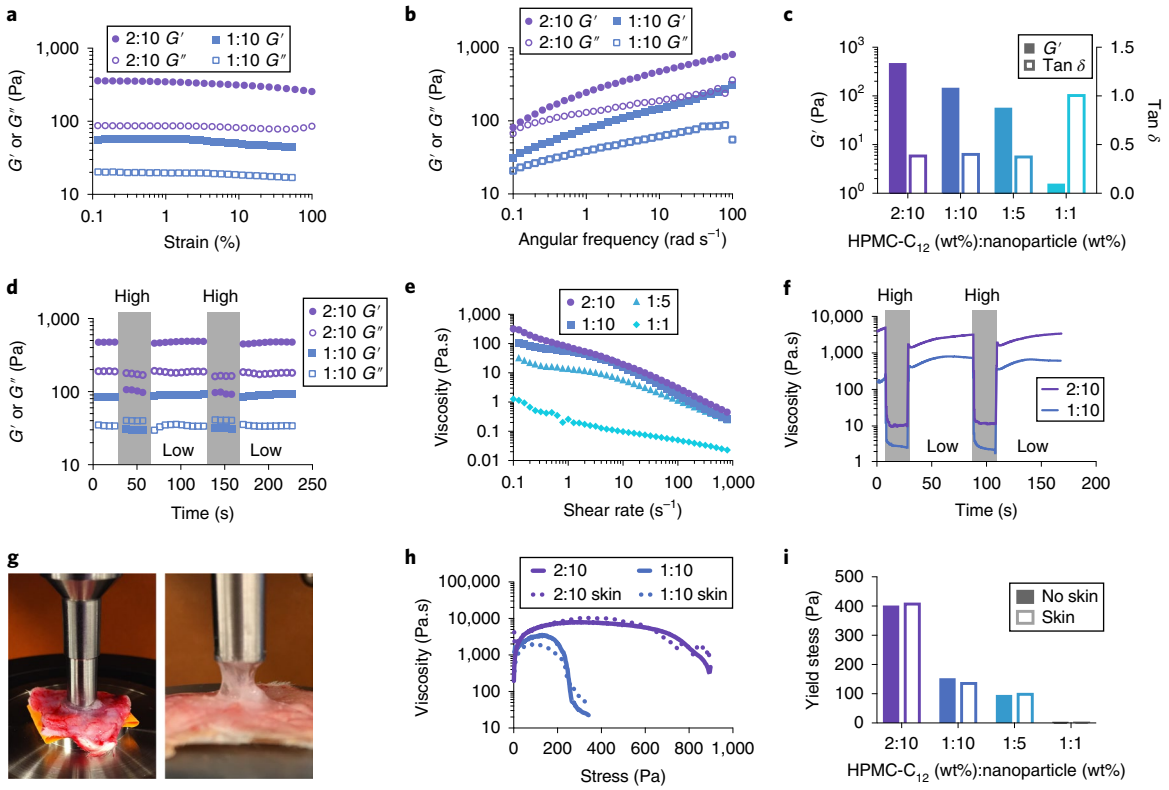

Fig. 2 | Mechanical characterization of PNP hydrogel adhesion barrier. a,**b**, Strain-dependent (**a**; $\omega = 10\,\mathrm{rad\,s^{-1}}$, 25 °C) and frequency-dependent (**b**; $\varepsilon = 2\%$, 25 °C) oscillatory shear rheology of PNP hydrogels comprising HPMC-C_{12} and PEG–PLA nanoparticles. **c**, Overview of oscillatory rheological properties of a series of PNP hydrogels ($\omega = 10\,\mathrm{rad\,s^{-1}}$, $\varepsilon = 2\%$, 25 °C). **d**, Step-strain measurements of PNP 1:10 and 2:10 hydrogel formulations with high strains (destructive; 750%) and low strains (restorative; 0.5%) to characterize extent and rate of stationary self-healing. **e**, Steady-shear rheology of various PNP hydrogel formulations demonstrating highly shear-thinning behaviour. **f**, Step-shear measurements of PNP 1:10 and 2:10 hydrogel formulations with high shear ($100\,\mathrm{s^{-1}}$) and low shear ($0.1\,\mathrm{s^{-1}}$) to characterize the extent and rate of flow-based self-healing. **g**, The experimental setup used to determine adhesion of PNP hydrogels to tissue (rat hypodermis). **h**, Yield stress behaviour of PNP 2:10 and 1:10 hydrogels in a standard parallel-plate geometry and on rat hypodermis in a stress-ramp experiment performed at a rate of approximately $1.5\,\mathrm{Pa\,s^{-1}}$. **i**, Yield stress values of PNP hydrogel formulations obtained from the peak viscosity observed in the stress ramp.

exhibited solid-like behaviour—that is, storage modulus (G') > loss modulus (G'')—and linear viscoelastic responses up to strains exceeding 100% in strain-dependent oscillatory rheological measurements (Fig. 2a). These results indicate that the hydrogels exhibit an extremely broad range of strains over which the solid-like properties are preserved. For reference, the highest strains experienced by tissues in the body are typically about 10% (ref. [44]); this means that the engineered material properties of the hydrogel are likely to be maintained in the dynamic environment in the body. Further, PNP hydrogels exhibited a frequency response that was highly dependent on the formulation in frequency-dependent oscillatory shear experiments performed in the linear viscoelastic regime (Fig. 2b). For comparison, the storage modulus (G') taken at frequency (ω) = $10\,\mathrm{rad\,s^{-1}}$ was used as a measure of hydrogel stiffness and the ratio tan $\delta = G''/G'$, taken at $\omega = 10\,\mathrm{rad\,s^{-1}}$ was used as a metric of hydrogel viscoelasticity (Fig. 2c). PNP 1:5, 1:10 and 2:10 maintained solid-like behaviour over the entire range of observed frequencies ($\omega = 0.1$ to $100\,\mathrm{rad\,s^{-1}}$), whereas PNP 1:1 and 0.2:10 were fluid-like. Step-strain measurements were performed to demonstrate recovery of the dynamic material response of the PNPs following network rupture at high strains. High-magnitude strain ($\varepsilon = 750\%$) was applied to break the hydrogel structure; this was followed by low magnitude strain ($\varepsilon = 0.5\%$) to investigate the rate and extent of hydrogel recovery to the initial mechanical properties (Fig. 3d). PNP 1:5, 1:10 and 2:10 hydrogels underwent a marked change to fluid-like behaviour at high strains, indicated by an inversion of G' and G'', but rapidly recovered (within 5 s) their initial solid-like dynamic response when the strain decreased. This behaviour was repeatable over several cycles, indicating that the shear thinning is driven by the rupture of the non-covalent crosslinks and not through cleavage of covalent bonds within the polymers.

Steady-shear and step-shear measurements were performed to investigate the flow properties of these materials, which are highly relevant to flow-based processes such as spraying, spreading or injection (Fig. 2e,f). PNP hydrogels were highly shear-thinning (Fig. 2e), reducing their viscosity by more than three orders of magnitude over shear rates extending from $0.1–100\,\mathrm{s^{-1}}$. The recovery of the mechanical properties of the PNP hydrogel following network rupture and flow at high shear rates, such as those imposed on the gel when spraying or injecting onto target tissues, were measured with step-shear experiments. High shear rates ($100\,\mathrm{s^{-1}}$) followed by low shear rates ($10\,\mathrm{s^{-1}}$) were applied to the hydrogel while monitoring the viscosity (Fig. 2f). Again, the PNP hydrogels showed marked shear-thinning at high shear rates, decreasing in viscosity by roughly three orders of magnitude, but quickly recovered their original viscosity when the shear rate was decreased. Similar to step-strain measurements discussed above, this rapid and complete recovery of mechanical properties was observed over several cycles.

The adhesion of PNP hydrogels to a model tissue, rat hypodermis, was characterized using yield-stress measurements (Fig. 2g). In these experiments, we determined the yield behaviour of PNP hydrogels alone in a standard geometry and on rat hypodermis.

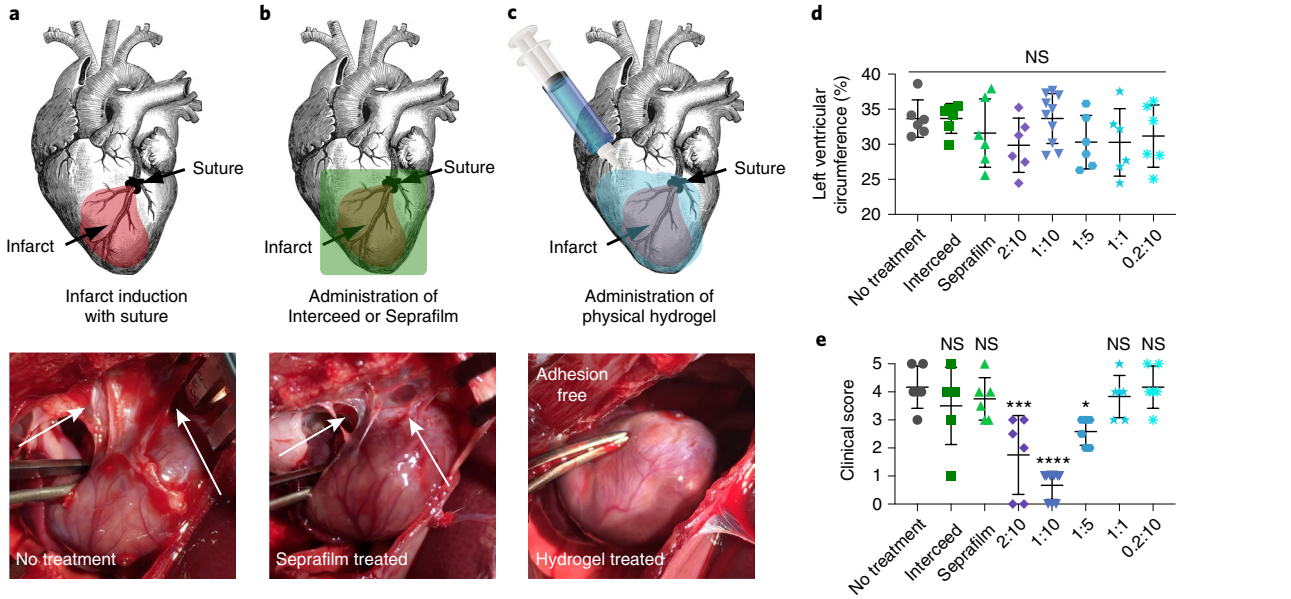

Fig. 3 | Prevention of pericardial adhesion in a rat model. a. Schematic illustration of induced myocardial infarction, whereby the LAD is ligated to prevent blood flow to the myocardium, leading to local myocardial infarction (top). Representative image ($n=6$) of an untreated control heart four weeks after infarction (bottom). **b**, Illustration of immediate administration of Interceed or Seprafilm following the infarction (top) and representative image ($n=6$) of a heart treated with a commercially available adhesion barrier (bottom), four weeks after infarction. **c**, Illustration of administration of PNP hydrogels immediately following infarction (top) and a representative image ($n=10$) of the in vivo efficacy of PNP hydrogel (1:10), four weeks after infarction. The white arrows indicate adhesions. **d**, Infarct size, expressed as percentage of left ventricle wall circumference, was used as a measure of induced local inflammation to ensure consistency across treatment and control groups. Data presented as mean ± s.d. ($n \geq 6$). **e**, Double-blinded clinical scoring of adhesion formation four weeks following induction of the myocardial infarction model. Data presented as mean ± s.d. ($n \geq 6$ per group). Statistical significance was determined using a one-way analysis of variance (ANOVA) with multiple comparisons against untreated controls. NS, not significant; $^{*}P=0.0156$, $^{***}P<0.001$ and $^{****}P<0.0001$; *n* refers to biological replicates.

We assumed that rat hypodermis would be an adequate predictor of PNP adhesion to tissues of interest such as epicardium, parietal pleura, mucosa and serosa, owing to the similarity of the tissues. For PNP 2:10 and 1:10 hydrogel formulations, the yield stress of the material is equivalent whether it is on tissue or not on tissue (Fig. 2h), indicative of a cohesive yielding behaviour (failure of the gel itself) and not adhesive failure between the hypodermis and gel (Fig. 2i). PNP 1:5, 1:10 and 2:10 hydrogels exhibited formulation-dependent yield stresses that were cohesive in nature, whereas PNP 1:1 did not exhibit a yield stress, probably owing to its fluid-like properties.

In vivo efficacy in a rat model of pericardial adhesion

To investigate the efficacy of the PNP hydrogel system, we created a reliable rat model of severe post-operative pericardial adhesions by inducing a myocardial infarction[45–50]. The inflammation and tissue damage occurring in this model reproducibly generated robust cardiac adhesions. The myocardial infarction model exhibited a greater incidence of severe adhesions, thus potentially providing a better predictor for a translationally relevant solution. An anterolateral myocardial infarction was induced in rats by permanent ligation of the left anterior descending coronary artery (LAD; Fig. 3a). Infarct size was controlled in all treatment groups by ligating the LAD at the same location in each surgery and visually assessing the extent of ventricular pallor before securing the suture knot.

Immediately following ligation, rats ($n=6$ per group) were randomized to receive either one of a series of PNP hydrogels (0.2:10, 1:1, 1:5, 1:10 or 2:10; 200 µl), commercially available adhesion barriers Interceed or Seprafilm (1 cm^2) or no treatment (that is, control) before closing the thoracotomy. Rats were euthanized four weeks later to evaluate the anti-adhesive efficacy. A sternotomy was performed to visualize adhesion formation and to assess the in vivo efficacy of the PNP hydrogel treatments (Fig. 3a–c). Using videos and images, adhesion scores were assigned using a standard, double-blinded clinical-scoring system on a scale from 0 to 5 (ref. [22]) (Fig. 3e and Supplementary Videos 1–8). The scoring system ranged from no adhesions (0), a few filmy adhesions (1), numerous filmy adhesions (2), moderate adhesions (3), dense adhesions (4) and very dense, vascularized adhesions (5). Finally, adhesions were removed and the heart was explanted for histological analysis. The infarct size was measured by the percentage of the left ventricular wall that was infarcted to ensure all animals experienced similar infarct sizes, inflammatory responses and tissue necrosis, which contribute to adhesion formation (Fig. 3d).

In the untreated control group, the hearts were completely adhered to the chest wall (Fig. 3a), presenting an adhesion score of 4.2 ± 0.8 (all results are shown as mean ± s.d.) and demonstrating the reliability of the myocardial infarction model in forming adhesions in the thoracic cavity. Commercial adhesion-barrier treatment groups presented with adhesion scores of 3.8 ± 0.8 and 3.3 ± 1.2, which were not statistically different from that of the control group (Fig. 3b). Rats treated with a PNP hydrogel adhesion barrier exhibited formulation-dependent adhesion scores, likely due to the differences in viscoelasticity and yield stress of the various materials investigated. Solid-like PNP hydrogel formulations ($G' > G''$) 1:5, 1:10 and 2:10 all formed physical adhesion barriers that significantly reduced the incidence and severity of adhesions when compared with the untreated control group, albeit with formulation-dependent efficacy and variability. By contrast, liquid-like PNP formulations ($G'' > G'$) 0.2:10 and 1:1 did not significantly inhibit adhesions, presumably owing to their propensity to flow under low stress.

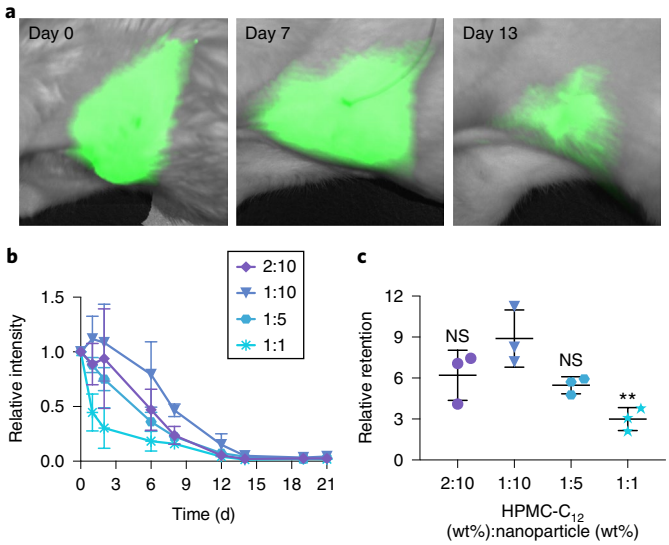

Fig. 4 | In vivo retention of PNP hydrogel adhesion barrier. a, Pearl live imaging of NIR-797-labelled PNP 1:10 hydrogel in the thoracic cavity following a thoracotomy, myocardial infarction and NIR-797-labelled PNP hydrogel administration. **b**, In vivo retention over time of the various PNP hydrogel formulations indicated by relative fluorescence intensity. **c**, Area under the curve values generated from the relative intensity curves in **b**. Data are presented as mean ± s.d. Statistical significance was determined by one-way ANOVA with multiple comparisons. NS, not significant; $^{**}P = 0.0055$; *n* refers to biological replicates.

PNP 1:10 performed the best as an adhesion barrier, as very minor adhesions were grossly observed, and animals presented with an adhesion score of 0.6 ± 0.5 ($P < 0.0001$) (Fig. 3c). The PNP 2:10 hydrogel also yielded a low mean adhesion score of 1.8 ± 1.4 ($P < 0.001$), but considerable variability in results was observed. Whereas PNP 1:5 hydrogel significantly reduced adhesions relative to the control group, with an adhesion score of 2.6 ± 0.4 ($P < 0.05$), it performed poorly when compared with the PNP 1:10 hydrogel group. These observations indicate that an optimal range of yield stress and/or storage moduli, as demonstrated by the PNP 1:10 hydrogel, results in more effective and sustained coverage of tissue over the four-week period, effectively preventing adhesions.

PNP hydrogel retention at the site of application

We hypothesized that the local retention time of the hydrogel in the cardiac space would be strongly correlated with robust tissue-adherence properties. The retention time frame of PNP 2:10, 1:10, 1:5 and 1:1 hydrogel formulations in the cardiac space following the thoracotomy was investigated with fluorescently labelled HPMC-C_{12} PNP hydrogels (Supplementary Fig. 2). Near-infrared (NIR) light sufficiently penetrates tissue to enable real-time imaging of the dye-labelled PNP hydrogels in the cardiac space over the four-week cardiac-adhesion-formation studies[51]. In these studies, rats were treated with NIR-797-labelled PNP hydrogels directly following vessel occlusion and imaged on day 0, 1, 2, 5, 7, 13, 16, 20 and 28 (Fig. 4). Following administration, hydrogels displayed intense signal in the pericardial space at the site of application (Fig. 4a). The signal steadily declined over the course of the study, indicating that the hydrogels persisted locally in the pericardial space for approximately two weeks (Fig. 4b). Since the reported pathophysiology for adhesion formation occurs 7–14 d after surgery, this time frame seems to be ideal for continual coverage and adhesion prevention in the thoracic cavity[52]. The overall relative retention for PNP 1:10 was significantly higher compared to the PNP 1:1 formulation (Fig. 4c). The increase in sustained retention in the PNP 1:10 group indicates a greater presence of material in the cardiac space over the course of the study. Due to the formulation dependency observed in the efficacy study, the overall material retention in the PNP 1:10 group seems to be beneficial for effective adhesion prevention.

PNP hydrogel biocompatibility

We hypothesized that a high degree of biocompatibility is required for effective adhesion prevention, because an inflammatory response from the adhesion barrier could lead to increased adhesion formation. Male rats underwent a sham surgery and received administration of 200 µl of PNP 1:10 hydrogel into the cardiac space or no treatment. At one week ($n = 5$ per group) and at four weeks ($n = 5$ per group) following surgery, rats were submitted to a pathologist and underwent complete necropsy for gross macroscopic findings. Surrounding tissues were explanted for microscopic histological analysis. A pathologist blinded to the treatment groups concluded that there were no substantial differences between the study groups. The major findings shared among both study groups included myofibre damage, fibrosis and inflammation in the thoracic wall. These observations are attributed to the thoracotomy and not the material itself. Complete blood count and blood chemistry panels also indicated no substantial abnormalities (Supplementary Fig. 3).

Large-animal model of epicardial abrasion

We conducted a pilot study using a preclinical translational sheep model to further investigate the efficacy of the PNP hydrogel anti-adhesion system and address the physiologic and anatomic differences between small animals and humans related to size and inflammatory response. We used an epicardial abrasion model (Fig. 5a–e), in which the anterior epicardial surface of the heart was abraded using a Bovie scratch pad for 30 s (Fig. 5a) to initiate an inflammatory response (Fig. 5b), resulting in the formation of severe adhesions. Animals ($n = 1$ per group) were randomized to receive Seprafilm (12 cm^2), PNP 1:10 hydrogel (25 ml) or no treatment. Seprafilm was chosen because it is the most commonly used of the commercially available adhesion-barrier products, and the PNP 1:10 hydrogel formulation was chosen because it exhibited the lowest adhesion score in the rat model.

PNP hydrogels could be easily sprayed onto the epicardial surface of the heart, enabling uniform coverage of the epicardial tissues. A 30 ml syringe was loaded with PNP hydrogel (25 ml) and attached to a Tisseel spray nozzle along with a compressed air line to provide the pressure necessary to spray the hydrogel onto the tissue (Fig. 5c,f, Supplementary Fig. 4 and Supplementary Video 9). Hydrogel application was completed in under 2 min. After the epicardial surface was completely coated with PNP 1:10 hydrogel (25 ml; Fig. 5g), the thoracotomy was closed. Seprafilm was applied as a sheet over the epicardial surface.

After four weeks, the sheep underwent median sternotomy and the pericardial adhesions were carefully released. The heart was dissected until all the major cardiac structures were exposed, including the left and right atrial appendage, left and right ventricle, LAD, main pulmonary artery, ascending aorta and the superior and inferior vena cavae. During this process, the surgeon assessed the severity of adhesions using the same double-blinded clinical-scoring system described in the rat study above. The region of interest for adhesion assessment was the anterior surface of the heart where the abrasion occurred. On completion of heart dissection, an image was captured and the heart was explanted. Figure 5h is a representative image of a human heart during redo surgery before heart dissection. This picture is provided to demonstrate the severity of adhesions observed in the clinical setting, which our model attempts to emulate. When comparing Fig. 5h with Fig. 5i, which shows an untreated sheep heart before dissection, there are severe adhesions present in both, demonstrating the ability of the abrasion model to generate robust adhesions. Figure 5j,l shows an attempt to release pericardial

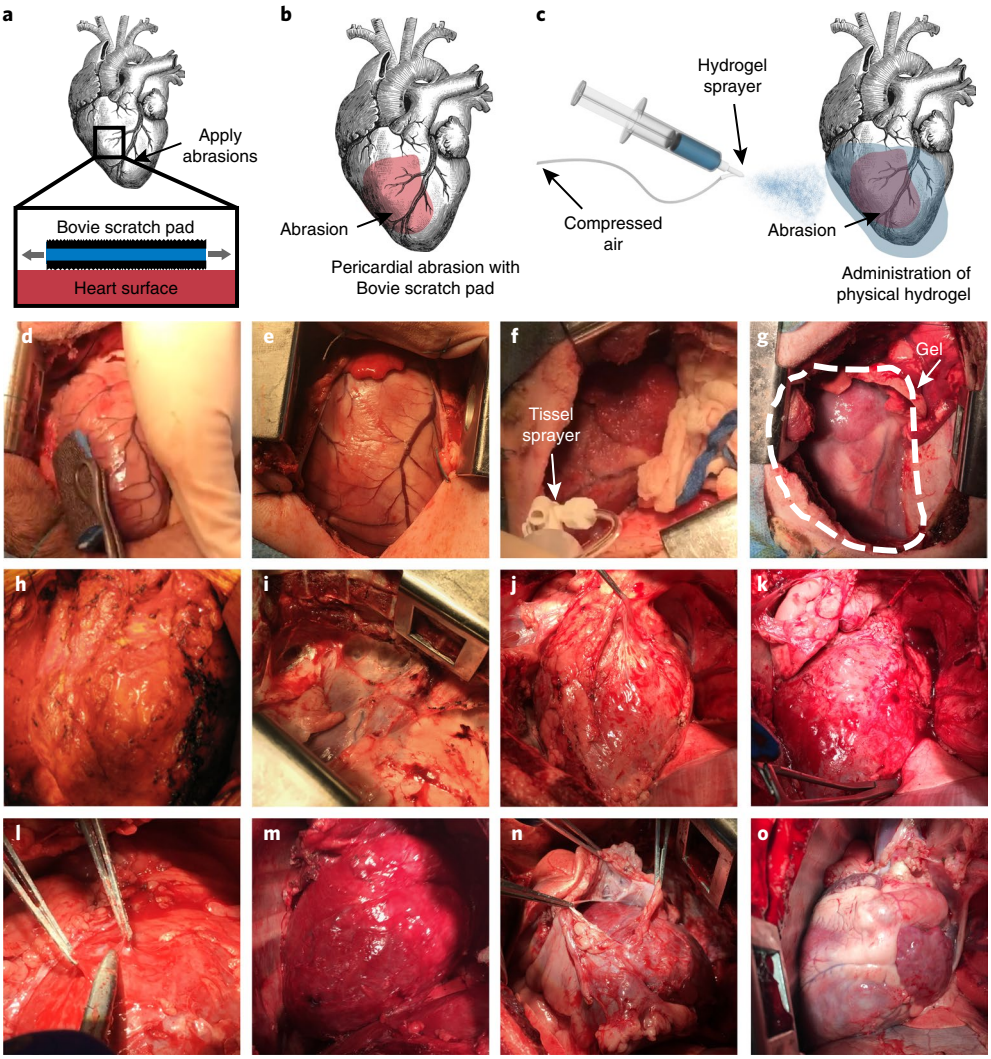

Fig. 5 | Prevention of adhesion in an epicardial abrasion model in sheep. a, Schematic representation of epicardial abrasion using a Bovie scratch pad. **b**, Schematic representation of epicardial abrasion to induce local inflammation, leading to formation of severe adhesions. **c**, Schematic representation of administration of PNP 1:10 hydrogel by spraying onto the heart. **d**,**e**, Sheep heart during epicardial abrasion (**d**) and immediately following abrasion showing inflamed ventricular tissue before closure (**e**). **f**, PNP 1:10 hydrogel being sprayed onto the epicardial surface. **g**, Image of PNP 1:10 hydrogel coating the epicardial surface immediately before closure. **h**, Representative image of a human heart during a redo surgery before heart dissection, showing ubiquitous and severe adhesions arising from the previous surgery. **i**, Image of adhesion formation in control sheep before heart dissection, indicating the presence of severe adhesions similar to those observed in humans and verifying the validity of the large-animal model. **j**, Pericardium and adhesion removal on a sheep heart four weeks following epicardial abrasion with no treatment. **k**, An untreated sheep heart after dissection. **l**. Pericardium and adhesion removal of a sheep heart four weeks after epicardial abrasion and treatment with Seprafilm. **m**, A sheep heart treated with Seprafilm following dissection. **n**, Pericardium removal four weeks following epicardial abrasion and treatment with PNP 1:10 hydrogel. **o**, A sheep heart treated with PNP 1:10 hydrogel following dissection, showing the absence of adhesions and a pristine, untouched appearance. Sample size for all groups is $n=1$.

adhesions from untreated and Seprafilm-treated hearts during the heart-dissection process. Pericardial adhesions were tightly adhered to the epicardial surface and could not be completely removed without excessive risk of damaging the heart. Figure 5k (untreated) and Fig. 5m (Seprafilm) show a substantial amount of tissue remaining on the epicardial surface as a result of tight adhesions. As a result of the pericardial adhesions, the untreated (Fig. 5k) and Seprafilm-treated (Fig. 5m) hearts closely resembled the human heart during a redo surgery and received severe adhesion scores of 4 and 5, respectively. By contrast, the PNP 1:10-treated heart appeared markedly different from those of the control and Seprafilm-treated groups and received an adhesion severity score of 0. Indeed, the pericardium could be lifted directly off the hydrogel-treated heart (Fig. 5n), revealing a pristine epicardial surface below (Fig. 5o). The dissection of the PNP hydrogel-treated heart was easier compared to that required for the control and Seprafilm-treated hearts, as all the major cardiac structures were completely and immediately visible after lifting the pericardium off the heart. Figure 5o shows the successful and complete removal of tissue surrounding the heart treated with PNP 1:10.

Cardiopulmonary bypass and aortotomy model

Next, we investigated the efficacy of the PNP hydrogel anti-adhesion system using a clinically relevant cardiopulmonary bypass and aortotomy model. Using central cannulation of the aortic arch and right atrium (Fig. 6a) and a pulmonary artery venting catheter to decompress the left ventricle, we performed a 2 cm partial transverse aortotomy on an arrested heart on cardiopulmonary bypass.

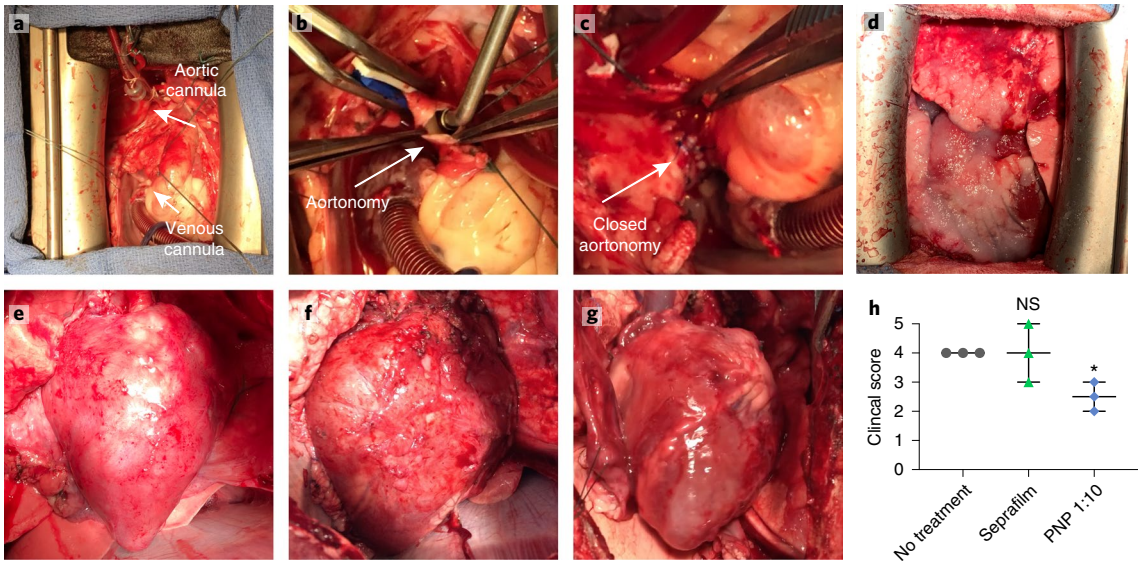

Fig. 6 | Sheep cardiopulmonary bypass and aortotomy model. a, Aortic arch and right atrium central cannulation and pulmonary artery venting catheter to decompress the left ventricle. **b**, Aortotomy performed to mimic standard aortic valve procedure. **c**, The closed aortotomy. **d**, The PNP 1:10 hydrogel coating the epicardial surface before closure. **e**, Representative image ($n=3$) of an untreated sheep heart after dissection. **f**, Representative image ($n=3$) of a sheep heart treated with Seprafilm, following dissection. **g**, Representative image ($n=3$) of a sheep heart treated with PNP 1:10 hydrogel, following dissection. **h**, Blinded clinical scoring of adhesion formation four weeks following cardiopulmonary bypass. Data presented as mean ± s.d. ($n=3$ per group). Statistical significance was determined using a two-tailed Student's *t*-test against untreated controls ($^*P=0.0065$). *n* refers to biological replicates.

The aortic valve was inspected to mimic a standard aortic valve surgery (Fig. 6b). The aortotomy was closed, the heart was reperfused and deaired, cardiopulmonary bypass was weaned off (Fig. 6c) and all cannulas were removed. Haemostasis was ensured at all surgical sites. At this point, sheep ($n=3$ per group) were randomized to receive Seprafilm (24 cm^2), PNP 1:10 hydrogel (50 ml) or no treatment. Similar to the epicardial abrasion model described above, PNP hydrogels were sprayed using compressed air and a spray nozzle (Fig. 6c,f) on the surface of the heart, including all surgical sites. After the heart surface was completely and uniformly coated with PNP 1:10 hydrogel (50 ml; Fig. 6d), the thoracotomy was closed. Seprafilm was applied as a sheet over the surface of the heart, including all surgical sites. Sheep underwent baseline and four-week magnetic resonance imaging to assess heart function and ensure consistency across treatment groups (Supplementary Fig. 5).

After four weeks, sheep underwent median sternotomy and the pericardial adhesions were released. Again, the heart was dissected until all the major cardiac structures were exposed, including all surgical and cannulation sites. During this process, the surgeon assessed the severity of adhesions using the same double-blinded clinical-scoring system described in the rat study and sheep epicardial abrasion study above. The region of interest for the adhesion assessment was the epicardial surface of the heart. On completion of heart dissection, an image was captured, the heart was explanted and the adhesion severity was scored. Figure 6e (untreated) and Fig. 6f (Sepraflim) show tissue remaining on the heart surface as a result of severe adhesion formation. Consequently, the untreated (Fig. 6e) and Seprafilm-treated (Fig. 6f) hearts received poor adhesion scores of 4 ± 0 and 4 ± 1, respectively. By contrast, the PNP 1:10-treated heart (Fig. 6g) resulted in much easier dissection, less severe adhesion formation and identifiable coronary vessels, resulting in a score of 2.5 ± 0.5 ($P<0.05$; Fig. 6h). Complete blood count and blood chemistry panels, conducted at four weeks, indicated no significant abnormalities between groups (Supplementary Fig. 6). These results demonstrate an effective, simple-to-apply adhesion-prevention system that reduces post-operative cardiac-adhesion formation in a clinically relevant cardiac-surgery model.

Discussion

This study demonstrates that a supramolecular polymeric hydrogel with complex viscoelastic and flow properties effectively prevents the formation of post-operative cardiac adhesions. These hydrogels exhibit the required shear-responsive rheological properties necessary for simple application (for example, by spraying) on target tissues, sustained local retention driven by strong tissue adherence and the formation of an effective viscoelastic barrier. This approach overcomes the limitations of traditional adhesion barriers that provide little-to-no therapeutic benefit and are often difficult to handle. PNP hydrogels are simple to manufacture at large scale, simple to deploy and demonstrate high efficacy in preventing adhesions, making them particularly well suited to potentially address this clinical challenge.

It is the distinct mechanical properties of the adhesion barrier that dictate its efficacy. While not all rheological possibilities for PNP hydrogels were investigated in this study, there are some key design parameters that appear to be necessary for a successful adhesion barrier. The material must be capable of viscous flow when shear is applied (for example, during spraying), enabling it to conform to and completely cover the target tissue. After the material is applied, it must rapidly take the form of a solid-like physical barrier that adheres to the tissue, does not delaminate and remains solid in the minimally perturbed environment near the heart. The material must be capable of flow between neighbouring body structures while remaining adhered to the tissue, allowing it to adjust to natural movement in the body. PNP hydrogels demonstrate this behaviour as yield stress fluids that are solid-like ($G'>G''$) below certain strains and stresses (Fig. 2e), but flow like viscous fluids above a critical stress–strain value, as shown in Fig. 2f. In addition, PNP hydrogels self-heal rapidly to reversibly transition from viscous flow back to a solid-like barrier, allowing the hydrogels to quickly adhere and settle on the target tissue.

The variation in clinical score between the PNP hydrogels demonstrates how modulus, viscoelasticity and the yield stress are critical for determining the effectiveness of the material as an adhesion barrier. Liquid-like formulations with their high tan δ at low strains and frequencies perform poorly because they never form a solid-like

barrier. Solid-like formulations show a correlation between the yield stress and storage modulus with the effectiveness as an adhesion barrier. The PNP 1:10 hydrogel formulation had the lowest adhesion score compared with the other gel formulations with an intermediate storage modulus and yield stress. We hypothesize that materials that are too soft and/or weak may flow too easily when perturbed in the body and leave the target tissue area too quickly while adhesions are still developing. Materials that are too stiff and/or strong may be more difficult to deposit, may easily detach from the tissue if the yield stress is higher than the adhesion strength, and may be more difficult to spread uniformly over a target area. Cohesive failure, which occurs when the yield stress is lower than the adhesion strength, enables the gel to be smeared or spread on the surface without delaminating, resulting in a barrier capable of being agitated without being removed from the tissue surface. This rationale is consistent with the variability observed in the adhesion score of PNP 2:10 hydrogel, where the increased yield strength may have prevented cohesive failure and led to more detachments of the gel from target tissues over the four-week study period.

Further studies are needed to optimize the PNP hydrogel system to further reduce cardiac adhesions in our large-animal model. Continued investigation with the cardiopulmonary-bypass sheep model will help to refine the most effective mechanical properties for adhesion prevention. We believe the cardiopulmonary-bypass model to be the most clinically relevant large-animal model due to the common use of cardiopulmonary bypass in human surgery. We attribute the the higher adhesion scores for the PNP hydrogel study group to the invasiveness of the procedure when compared with the pilot epicardial abrasion study. Cardiopulmonary bypass also induces a greater systemic inflammatory response, which is different from the local inflammatory response induced in the epicardial abrasion model that could also contribute to the difference in adhesion scores. We believe this anti-adhesion PNP hydrogel system has the potential to be effective in many surgical indications in many parts of the body. Furthermore, the easy and scalable synthesis of the PNP hydrogel system makes it amenable to preparation with good manufacturing practices, which is critical for future clinical translation of this work. Our hydrogel adhesion barrier produced a substantial reduction in both incidence and severity of cardiac adhesions, using models that generate adhesions of greater severity than those seen in abdominal-adhesion models. Overall, our shear-thinning and self-healing adhesion barrier establishes the proof-of-concept for a technology that is simple to deploy and successfully prevents post-operative adhesions.

Methods

Materials. HPMC-C12, *N*,*N*-diisopropylethylamine (Hunig's base) hexanes, diethyl ether, *N*-methylpyrrolidone (NMP), dichloromethane, lactide and diazobicylcoundecene (DBU) were purchased from Sigma-Aldrich and used as received.

Synthesis of HPMC-C_{12}. HPMC-C_{12} was prepared as previously described[34] and the methods are reproduced here. HPMC (1.0 g) was dissolved in NMP (40 ml) by stirring at 80 °C for 1 h. Once the solution cooled to room temperature, 1-dodecylisocynate (105 mg, 0.5 mmol) and *N*,*N*-diisopropylethylamine (catalyst, ~3 drops) were dissolved in NMP (5.0 ml). This solution was added to the reaction mixture, which was then stirred at room temperature for 16 h. This solution was then precipitated from acetone and the polymer was recovered by filtration, dried under vacuum at room temperature for 24 h and weighed, yielding functionalized HPMC-C_{12} as a white amorphous powder.

Synthesis of PEG-b-PLA. PEG-b-PLA was prepared as previously described[34] and the methods are reproduced here. PEG (0.25 g, 4.1 mmol; Aldrich) and DBU (10 µl, 10.6 mg; 1.0 mol% relative to lactide) were dissolved in dichloromethane (1.0 ml). Lactide (1.0 g, 6.9 mmol) was dissolved in dichloromethane (3.0 ml) with mild heating. The lactide solution was added rapidly to the PEG–DBU solution and was allowed to stir for 10 min. The reaction mixture was quenched and precipitated with 1:1 hexane and ethyl ether solution. PEG-b-PLA was collected and dried under vacuum.

PEG-b-PLA nanoparticle preparation. PEG–PLA nanoparticles were prepared as previously described[34] and the methods are reproduced here. A solution of PEG-b-PLA in DMSO (50 mg ml^{-1}) was added dropwise to water (80 µl min^{-1}) under a high stir rate. Nanoparticles were purified by ultracentrifugation over a filter (molecular weight cut-off of 10 kDa; Millipore Amicon Ultra-15) followed by resuspension in water to a final concentration of 150 mg ml^{-1}. Nanoparticle size and dispersity were characterized by dynamic light scattering (DLS).

PNP hydrogel preparation. PNP hydrogels were prepared by first dissolving HPMC polymers in water (3 wt% or 6 wt%) with stirring and mild heating. PEG–PLA nanoparticles were prepared according to the method described above and were concentrated to 15 wt% solutions. HPMC polymer solution (150 ml) and nanoparticle solution (300 ml) were added together and mixed well by vortexing (some samples were mildly centrifuged to remove bubbles arising from mixing) to create the PNP 1:10 hydrogel formulation. For each subsequent hydrogel formulation, the amount of HPMC polymer solution and NP solution was varied as indicated by the given formulation name (HPMC (wt%):NP (wt%)).

PNP hydrogel characterization. Rheological characterization was performed using a TA Instruments HR-2 hybrid rheometer fitted with a Peltier stage. All measurements were performed using a 20 mm plate or 8 mm plate geometry and analysed using TA Instruments TA Orchestrator software.

NIR-797-labelled HPMC-C_{12} preparation. NIR-797-labelled HPMC-C_{12} (excitation wavelength = 795 nm; emission wavelength = 817 nm) was prepared using a modification of a previously described method[53]. Sixty milligrams of HPMC-C_{12} was dissolved in 1.6 ml NMP containing 10 µl pyridine. Five milligrams of NIR-797 isothiocyanate (Sigma) was added to the solution, followed by 4 mg of dibutyltin dilaurate and was left stirring for a minimum of 4 h. The mixture was precipitated into acetone to remove free dye and NIR-797–HPMC-C_{12} was dried in vacuo. The NIR-797–HPMC-C_{12} was dialysed for four days to remove impurities and then freeze-dried. The NIR-797–HPMC-C_{12} sample was dissolved in MilliQ water at 3 wt% concentration and the fluorescence intensity was measured at 800 nm.

Rat pericardial adhesion model. All animal procedures were performed according to Stanford Animal Care and Use Committee approved protocols. For in vivo efficacy studies, 52 male adult 250–300 g Sprague Dawley rats (Charles River) underwent an induced myocardial infarction using an established and highly reproducible model[49]. In brief, rats were anaesthetised in an induction chamber and 2% isoflurane was continuously delivered. Rats were endotracheally intubated with a 16-gauge angiocatheter and mechanically ventilated (Hallowell EMC) with 2% isoflurane. A thoracotomy was performed, the heart was exposed and a 6-0 polypropylene suture was used to permanently ligate the LAD 2 mm below the left atrial appendage, producing an anterolateral myocardial infarction. Immediately following ligation, the epicardial surface was dried and the rats received administration of PNP 0.2:10 (n = 6), 1:1 (n = 6), 1:5 (n = 6), 1:10 (n = 10) or 2:10 (n = 6) hydrogels (200 µl); Interceed (n = 6); Seprafilm (n = 6) (commercially available standard-of-care adhesion barriers; 1 cm^2); or no treatment (n = 6). A subset of rats was administered PNP 1:10 hydrogel for the in vivo retention study. The thoracotomy was closed with 4-0 polypropylene suture. The rats were allowed to recover and buprenorphine (0.5 mg kg^{-1}) and carprofen (5 mg kg^{-1}) were given for analgesia.

In vivo retention study. A subset of rats was administered NIR-797-tagged PNP hydrogels immediately following the induced myocardial infarction. Rats were imaged on day 0, 1, 2, 5, 7, 13, 16, 20 and 28 using the Pearl Trilogy Small Animal Imaging System (LI-COR Biosciences).

Histology. Four weeks after surgery, hearts were arrested with potassium chloride and explanted to assess infarct size and tissue biocompatibility. Hearts were flushed with PBS, injected retrogradely with Tissue Tek optimum cutting temperature (OCT) compound (Sekura), frozen, stored at −80 °C and sectioned onto slides using a Leica CM3050S cryostat (Leica) at 10 µm thickness. A subset of samples for each group was stained with Masson's trichrome. Digital photographs were taken with an Epson V550 Colour Scanner. Images were analysed with ImageJ and infarct size was calculated as the percentage of the total left ventricular circumference.

Biocompatibility study. All animal procedures were performed according to Stanford Animal Care and Use Committee approved protocols. For biocompatibility studies, 20 adult 250–300 g Sprague Dawley rats (Charles River) underwent a sham surgery. In brief, rats were anaesthetized in an induction chamber and 2% isoflurane was continuously delivered. Rats were endotracheally intubated with a 16-gauge angiocatheter and mechanically ventilated (Hallowell EMC) with 2% isoflurane. A thoracotomy was performed and the heart was exposed. The pericardium was removed, the epicardial surface was dried and the rats received PNP 1:10 (n = 10) or no treatment (n = 10). The thoracotomy was closed with 4-0 polypropylene suture. The rats were allowed to recover and

buprenorphine (0.5 mg kg^{-1}) and carprofen (5 mg kg^{-1}) were given for analgesia. At one week and four weeks, a subset of animals ($n = 5$ per group) was submitted to a pathologist for complete necropsy and histologic analysis. Complete blood counts and blood chemistry tests were also conducted at these time points. The tissues explanted and sectioned for histological analysis were liver, spleen, kidney, adrenal gland, salivary gland, thymus, pancreas, heart, lung, trachea, oesophagus, thyroid gland, tongue, lymph nodes, testes, accessory sex gland, eyes, cerebrum, cerebellum, stomach, small intestine, large intestine and thoracic wall. There was one block per organ and two sections per slide per rat.

Sheep epicardial abrasion adhesion model. All animal procedures were performed according to Stanford Animal Care and Use Committee approved protocols. For pilot epicardial abrasion efficacy studies, 3 adult male 35–45 kg Dorset sheep underwent epicardial abrasion to induce pericardial-adhesion formation. In brief, the animals were sedated with diazepam (0.2 mg kg^{-1}) and anaesthesia was maintained on inhaled isoflurane (1.5–3%). A 5 cm minimally invasive left thoracotomy was used to access the chest cavity and the heart was exposed. The anterior wall of the heart was abraded for 30 seconds, creating an inflamed area of epicardium. Animals were randomized to receive PNP 1:10 hydrogel (25 ml), Seprafilm (12 cm^2) or no treatment. The thoracotomy was closed. The animals were allowed to recover from anaesthesia and buprenorphine (0.05 mg kg^{-1}) was given intramuscularly for post-operative pain control. All surviving animals were euthanized 4 weeks following pericardial abrasion to access for adhesion formation.

Sheep cardiopulmonary bypass adhesion model. All animal procedures were performed according to Stanford Animal Care and Use Committee approved protocols. For cardiopulmonary bypass adhesion studies, 9 adult male 35–45 kg Dorset sheep underwent cardiopulmonary bypass and an aortonomy to induce adhesion formation. In brief, the animals were sedated with diazepam (0.2 mg kg^{-1}) and anaesthesia was maintained on inhaled isoflurane (1.5–3%). A 7 cm left thoracotomy was used to access the chest cavity and the heart was exposed.

A double-pledgeted pursestring suture (2-0 Ethibond) was placed on the aortic arch. A single-pledgeted pursestring suture (2-0 Ethibond) was placed on the right atrial appendage. Heparin was administered (11,000 units). A 16 Fr aortic cannula was inserted using Seldinger technique into the aortic arch and a 30 Fr single-stage venous cannula was inserted into the right atrium. The cannulae were connected to the cardiopulmonary bypass circuit. Cardiopulmonary bypass was initiated. A pulmonary-artery venting catheter was placed into the main pulmonary artery to decompress the left ventricle. An aortic cross-clamp was applied. A cardioplegia needle was placed into the ascending aorta and cold Del Nido cardioplegia (500–1,000 cm^3) was administered to arrest the heart. The cardioplegia needle was removed. A 2 cm partial transverse aortotomy was made and the aortic valve was inspected. The aortotomy was then closed using 5-0 polypropylene suture. The heart was filled and de-aired. The cross clamp was removed and the heart spontaneously resumed a normal rhythm. The pulmonary artery vent was removed and the vent site was repaired primarily using 5-0 polypropylene suture. Cardiopulmonary bypass was weaned. Finally, the right atrial and aortic arch cannulae were removed. Protamine (100 mg) was administered. Haemostasis was achieved for all surgical sites using Surgicell as needed.

Sheep were randomized to receive administration of PNP 1:10 hydrogel (50 ml), Seprafilm (24 cm^2) or no treatment. The thoracotomy was closed. The animals were allowed to recover from anaesthesia and buprenorphine (0.05 mg kg^{-1}) was used for post-operative pain control. All surviving animals were euthanized four weeks following pericardial abrasion to access adhesion formations.

Statistical analysis. All results are expressed as mean ± s.d. Comparison between two groups were conducted by a two-tailed Student's *t*-test. One-way ANOVA was used for comparisons across multiple groups. Statistical significance was considered as $P < 0.05$.

Animal randomization. Animal cages for rats and sheep were housed in a random order on the shelf. Physical randomization occurred before each operation using a random number generator. The adhesion scoring and heart explants were done in a random order, with the surgeon and clinical scorer being blinded to the treatment groups.

Reporting summary. Further information on research design is available in the Nature Research Reporting Summary linked to this article.

Data availability

The main data supporting the results in this study are available within the paper and its Supplementary Information. The raw and analysed datasets generated during the study are available for research purposes from the corresponding authors on reasonable request.

Received: 8 May 2018; Accepted: 8 July 2019;
Published online: 7 August 2019

References

1. Lauder, C. I., Garcea, G., Strickland, A. & Maddern, G. J. Abdominal adhesion prevention: still a sticky subject? *Dig. Surg.* **27**, 347–358 (2010).
2. Weibel, M. A. & Majno, G. Peritoneal adhesions and their relation to abdominal surgery. A postmortem study. *Am. J. Surg.* **126**, 345–353 (1973).
3. DiZerega, G. S. in *Peritoneal Surgery* (ed. DiZerega, G. S.) 3–37 (Springer, 2000).
4. Ito, T. et al. The prevention of peritoneal adhesions by in situ cross-linking hydrogels of hyaluronic acid and cellulose derivatives. *Biomaterials* **28**, 975–983 (2007).
5. Yea, Y. et al. Prevention of peritoneal adhesions with an in situ cross-linkable hyaluronan hydrogel delivering budesonide. *J. Control. Release* **120**, 178–185 (2007).
6. Hirschelmann, A., Tchartchian, G., Wallwiener, M., Hackethal, A. & De Wilde, R. L. A review of the problematic adhesion prophylaxis in gynaecological surgery. *Arch. Gynecol. Obstet.* **285**, 1089–1097 (2012).
7. Shahian, D. M. et al. The society of thoracic surgeons 2008 cardiac surgery risk models: part 1—coronary artery bypass grafting surgery. *Ann. Thorac. Surg.* **88**, S2–S22 (2009).
8. O'Brien, S. M. et al. The Society of thoracic surgeons 2008 cardiac surgery risk models: part 2—isolated valve surgery. *Ann. Thorac. Surg.* **88**, S23–S42 (2009).
9. Kansara, P. et al. Heart transplantation with and without prior sternotomy: analysis of the united network for organ sharing database. *Transpl. Proc.* **46**, 249–255 (2014).
10. Hoffman, J. L. et al. The incidence of congenital heart disease. *J. Am. Coll. Cardiol.* **39**, 1890–1900 (2002).
11. Jacobsa, J. P. et al. Reoperations for pediatric and congenital heart disease: An analysis of the society of thoracic surgeons (STS) congenital heart surgery database. *Semin. Thorac. Cardiovasc. Surg. Pediatr. Card. Surg. Annu.* **17**, 2–8 (2014).
12. Sikirica, V. et al. The inpatient burden of abdominal and gynecological adhesiolysis in the US. *BMC Surgery* **11**, 1–9 (2011).
13. Diamond, M. P., Burns, E. L., Accomando, B., Mian, S. & Holmdahl, L. Seprafilm adhesion barrier: (1) a review of preclinical, animal, and human investigational studies. *Gynecol. Surg.* **9**, 237–245 (2012).
14. Malm, T., Bowald, S., Bylock, A. & Busch, C. Prevention of postoperative pericardial adhesions by closure of the pericardium with absorbable polymer patches. An experimental study. *J. Thorac. Cardiovasc. Surg.* **104**, 600–607 (1992).
15. Duncan, D. A. et al. Prevention of postoperative pericardial adhesions with hydrophilic polymer solutions. *J. Surg. Res.* **45**, 44–49 (1987).
16. Seeger, J. M. et al. Prevention of postoperative pericardial adhesions using tissue-protective solutions. *J. Surg. Res.* **68**, 63–66 (1997).
17. Hoare, T., Yeo, Y., Bellas, E., Bruggeman, J. P. & Kohane, D. S. Prevention of peritoneal adhesions using polymeric rheological blends. *Acta Biomater.* **10**, 1187–1193 (2014).
18. Yeo, Y. & Kohane, D. S. Polymers in the prevention of peritoneal adhesions. *Eur. J. Pharm. Biopharm.* **68**, 57–66 (2008).
19. Grainger, D. A., Meyer, W. R., DeCherney, A. H. & Diamond, M. P. The use of hyaluronic acid polymers to reduce postoperative adhesions. *J. Gynecol. Surg.* **7**, 97–101 (2009).
20. Sawhney, A. S., Pathak, C. P., Van Rensburg, J. J., Dunn, R. C. & Hubbell, J. A. Optimization of photopolymerized bioerodible hydrogel properties for adhesion prevention. *Biomed. Mater. Res.* **28**, 831–838 (1994).
21. Connors, R. C. et al. Postoperative pericardial adhesion prevention using carbylan-SX in a rabbit model. *J. Surg. Res.* **140**, 237–242 (2007).
22. Li, L. et al. Biodegradable and injectable in situ cross-linking chitosan-hyaluronic acid based hydrogels for postoperative adhesion prevention. *Biomaterials* **35**, 903–3917 (2014).
23. Zhu, W. et al. Metal and light free 'click' hydrogels for prevention of post-operative peritoneal adhesions. *Polym. Chem.* **5**, 2018–2026 (2014).
24. Chan, M. et al. Reducing the oxidation level of dextran aldehyde in a chitosan/dextran-based surgical hydrogel increases biocompatibility and decreases antimicrobial efficacy. *Int. J. Mol. Sci.* **16**, 13798–13814 (2015).
25. Song, L. et al. Peritoneal adhesion prevention with a biodegradable and injectable N,O-carboxymethyl chitosan-aldehyde hyaluronic acid hydrogel in a rat repeated-injury model. *Sci. Rep.* **6**, 37600 (2016).
26. Yang, Y. et al. A postoperative anti-adhesion barrier based on photoinduced imine-crosslinking hydrogel with tissue-adhesive ability. *Acta Biomater.* **62**, 199–209 (2017).
27. Banasiewicz, T. et al. Preliminary study with SprayShieldadhesion barrier system in the prevention of abdominal adhesions. *Video. Mini.* **8**, 301–309 (2013).
28. Napoleone, C. et al. An observational study of CoSeal for the prevention of adhesions in pediatric cardiac surgery. *Inter. Cardiovasc. Thorac. Surg.* **9**, 978–982 (2009).
29. Haensig, M. et al. Bioresorbable adhesion barrier for reducing the severity of postoperative cardiac adhesions: Focus on REPEL-CV. *Med. Devices* **4**, 17–25 (2011).

30. Hirschelmann, A. et al. Is patient education about adhesions a requirement in abdominopelvic surgery? *Geburtshilfe Frauenheilkd.* **72**, 299–304 (2012).
31. Wang, Q. et al. High-water-content mouldable hydrogels by mixing clay and a dendritic molecular binder. *Nature* **463**, 339–343 (2010).
32. Appel, E. A., Barrio, J., Loh, X. J. & Scherman, O. A. Supramolecular polymeric hydrogels. *Chem. Soc. Rev.* **41**, 6195–6214 (2012).
33. Rose, S. et al. Nanoparticle solutions as adhesives for gels and biological tissues. *Nature* **505**, 382–385 (2014).
34. Appel, E. A. et al. Self-assembled hydrogels utilizing polymer–nanoparticle interactions. *Nat. Commun.* **4**, 848–852 (2015).
35. Rodell, C. B. et al. Shear-thinning supramolecular hydrogels with secondary autonomous covalent crosslinking to modulate viscoelastic properties. *Adv. Funct. Mater.* **25**, 636–644 (2015).
36. Webber, M. J. et al. Supramolecular biomaterials. *Nat. Mater.* **15**, 13–26 (2015).
37. Appel, E. A. et al. Supramolecular cross-linked networks via host–guest complexation with cucurbit[8]uril. *J. Am. Chem. Soc.* **132**, 14251–14260 (2010).
38. Appel, E. A. et al. High-water-content hydrogels from renewable resources through host-guest interactions. *J. Am. Chem. Soc.* **134**, 11767–11773 (2012).
39. Appel, E. A. et al. Sustained release of proteins from high water content supramolecular hydrogels. *Biomaterials* **33**, 4646–4652 (2012).
40. Appel, E. A. et al. Activation energies control macroscopic properties of physically crosslinked materials. *Angew. Chem. Int. Ed.* **53**, 10038–10043 (2014).
41. Appel, E. A. et al. The control of cargo release from physically crosslinked hydrogels by crosslink dynamics. *Biomaterials* **35**, 9897–9903 (2014).
42. Appel, E. A. & Scherman, O. A. Gluing gels: A nanoparticle solution. *Nat. Mater.* **13**, 231–232 (2014).
43. Yu, A. C. et al. Scalable manufacturing of biomimetic moldable hydrogels for industrial applications. *Proc. Natl Acad. Sci. USA* **113**, 14255–14260 (2016).
44. Evans, N. D., Oreffo, R. O., Healy, E., Thurner, P. J. & Man, Y. H. Epithelial mechanobiology, skin wound healing, and the stem cell niche. *J. Mech. Behav. Biomed. Mater.* **28**, 397–409 (2013).
45. Arung, W., Meurisse, M. & Detry, O. Pathophysiology and prevention of postoperative peritoneal adhesions. *World J. Gastroenterol.* **17**, 4545–4553 (2011).
46. Alizzi, A. M. et al. Reduction of post-surgical pericardial adhesions using a pig model. *Heart Lung Circ.* **21**, 22–29 (2012).
47. Lassaletta, A. D., Chu, L. M. & Selke, F. W. Effects of alcohol on pericardial adhesion formation in hypercholesterolemic swine. *J. Thorac. Cardiovasc. Surg.* **143**, 953–959 (2012).
48. Lassaletta, A. D. et al. Mechanism for reduced pericardial adhesion formation in hypercholesterolemic swine supplemented with alcohol. *Eur. J. Cardiothorac. Surg.* **43**, 1058–1064 (2013).
49. Macarthur, J. W. et al. Preclinical evaluation of the engineered stem cell chemokine stromal cell-derived factor 1α analog in a translational ovine myocardial infarction model. *Circ. Res.* **114**, 650–659 (2014).
50. Elmadhun, N. Y. et al. Effects of alcohol on postoperative adhesion formation in ischemic myocardium and pericardium. *Ann. Thorac. Surg.* **104**, 545–552 (2017).
51. MacArthur, J. W. et al. Sustained release of engineered stromal cell-derived factor 1-α from injectable hydrogels effectively recruits endothelial progenitor cells and preserves ventricular function after myocardial infarction. *Circulation* **128**, S79–S86 (2013).
52. DiZerega, G. S. et al. Peritoneal repair and post-surgical adhesion formation. *Hum. Reprod.* **6**, 547–555 (2001).
53. Yashiharu, K. et al. Pharmacokinetics and biodisposition of poly(vinyl alcohol) in rats and mice. *Drug Metab. Pharmacokinet.* **20**, 435–442 (2005).

Acknowledgements

This work was made possible by the financial support from the Stanford BIOX Interdisciplinary Initiatives Program Seed Grant (E.A.A. and Y.J.W.), the Stanford-Coulter Translational Research Grant (E.A.A. and Y.J.W.), the National Institutes of Health (R01HL089315-01, Y.J.W.), the American Heart Association postdoctoral fellowship (H.W. and M.J.P.) and predoctoral fellowship (L.M.S.), the National Science Foundation AGEP California Alliance Postdoctoral Fellowship (H.L.H.) and Graduate Research Fellowship Program (DGE-1147470, L.M.S., A.N.S. and G.A.), the Stanford Interdisciplinary Graduate Fellowship (L.M.S.), and the American Association for Thoracic Surgery Summer Intern Scholarship (K.M.W.). The authors thank the Bogyo laboratory for the use of the Pearl instrument, the Stanford Veterinary Services Center for assistance with ovine surgeries and the Stanford Animal Histology Services for assistance with histology.

Author contributions

L.M.S., A.N.S., A.C.Y., H.W., M.J.P., A.A.A.S., Y.J.W. and E.A.A. designed experiments; L.M.S., H.W., H.J.L., A.D.T., H.L.H., G.A., K.P.T. and E.A.A. conducted experiments; J.M.F., H.J.L., A.D.T., A.E., K.M.W., C.E.H., K.J.J., M.J.P., S.W.B., B.C., C.M., F.G., H.B. and M.M. assisted with ovine surgeries; L.M.S., A.N.S., Y.T., Y.J.W. and E.A.A. analysed data; and L.M.S., Y.J.W. and E.A.A. wrote the paper.

Competing interests

The authors declare no competing interests.

Additional information

Supplementary information is available for this paper at https://doi.org/10.1038/s41551-019-0442-z.

Reprints and permissions information is available at www.nature.com/reprints.

Correspondence and requests for materials should be addressed to E.A.A. or Y.J.W.

Publisher's note: Springer Nature remains neutral with regard to jurisdictional claims in published maps and institutional affiliations.

nature research

Corresponding author(s): Eric Appel and Joseph Woo

Last updated by author(s): Jun 18, 2019

Reporting Summary

Nature Research wishes to improve the reproducibility of the work that we publish. This form provides structure for consistency and transparency in reporting. For further information on Nature Research policies, see Authors & Referees and the Editorial Policy Checklist.

Statistics

For all statistical analyses, confirm that the following items are present in the figure legend, table legend, main text, or Methods section.

n/a	Confirmed	
☐	☒	The exact sample size (*n*) for each experimental group/condition, given as a discrete number and unit of measurement
☐	☒	A statement on whether measurements were taken from distinct samples or whether the same sample was measured repeatedly
☐	☒	The statistical test(s) used AND whether they are one- or two-sided *Only common tests should be described solely by name; describe more complex techniques in the Methods section.*
☐	☒	A description of all covariates tested
☐	☒	A description of any assumptions or corrections, such as tests of normality and adjustment for multiple comparisons
☐	☒	A full description of the statistical parameters including central tendency (e.g. means) or other basic estimates (e.g. regression coefficient) AND variation (e.g. standard deviation) or associated estimates of uncertainty (e.g. confidence intervals)
☐	☒	For null hypothesis testing, the test statistic (e.g. *F*, *t*, *r*) with confidence intervals, effect sizes, degrees of freedom and *P* value noted *Give P values as exact values whenever suitable.*
☒	☐	For Bayesian analysis, information on the choice of priors and Markov chain Monte Carlo settings
☒	☐	For hierarchical and complex designs, identification of the appropriate level for tests and full reporting of outcomes
☒	☐	Estimates of effect sizes (e.g. Cohen's *d*, Pearson's *r*), indicating how they were calculated

Our web collection on statistics for biologists contains articles on many of the points above.

Software and code

Policy information about availability of computer code

Data collection	No software was used.
Data analysis	Prism 7 and Prism 8.

For manuscripts utilizing custom algorithms or software that are central to the research but not yet described in published literature, software must be made available to editors/reviewers. We strongly encourage code deposition in a community repository (e.g. GitHub). See the Nature Research guidelines for submitting code & software for further information.

Data

Policy information about availability of data

All manuscripts must include a data availability statement. This statement should provide the following information, where applicable:

- Accession codes, unique identifiers, or web links for publicly available datasets
- A list of figures that have associated raw data
- A description of any restrictions on data availability

The authors declare that the main data supporting the results in this study are available within the paper and its Supplementary Information. The raw and analysed datasets generated during the study are available for research purposes from the corresponding authors on reasonable request.

Field-specific reporting

Please select the one below that is the best fit for your research. If you are not sure, read the appropriate sections before making your selection.

☒ Life sciences ☐ Behavioural & social sciences ☐ Ecological, evolutionary & environmental sciences

Life sciences study design

All studies must disclose on these points even when the disclosure is negative.

Sample size	Sample size of n=6 for the rodent cardiac adhesion study was determined from a calculated study power of greater than 0.80. No sample size calculation was performed for the ovine-bypass-model study; however, the sample size of n=3 for the ovine bypass model was sufficient to yield a study power of greater than 0.80.
Data exclusions	Animals that were part of the survival surgical learning curve were excluded from the data.
Replication	The rodent cardiac adhesion study was performed once with 6 or more animals in each group. The rodent in vivo retention study was performed once with 3 animals per group. The rodent biocompatibility study was performed once with 5 animals in each group. The ovine cardiopulmonary bypass study was performed once with 3 animals per group. The results in this manuscript were reliably reproduced between biological replicates.
Randomization	Animals were chosen for each treatment group at random, by using a random-number generator.
Blinding	Investigators were blinded to the treatment groups during adhesion severity scoring and tissue histological analysis.

Reporting for specific materials, systems and methods

We require information from authors about some types of materials, experimental systems and methods used in many studies. Here, indicate whether each material, system or method listed is relevant to your study. If you are not sure if a list item applies to your research, read the appropriate section before selecting a response.

Materials & experimental systems

n/a	Involved in the study
☒	☐ Antibodies
☒	☐ Eukaryotic cell lines
☒	☐ Palaeontology
☐	☒ Animals and other organisms
☒	☐ Human research participants
☒	☐ Clinical data

Methods

n/a	Involved in the study
☒	☐ ChIP-seq
☒	☐ Flow cytometry
☒	☐ MRI-based neuroimaging

Animals and other organisms

Policy information about studies involving animals; ARRIVE guidelines recommended for reporting animal research

Laboratory animals	Male Sprague Dawley Rats from Charles River between 3–4 months old, 250–300g, were used for rodent studies. Male Dorset sheep 35–45kg were used for the ovine studies.
Wild animals	The study did not involve wild animals.
Field-collected samples	The study did not involve samples collected from the field
Ethics oversight	All animal procedures were performed according to protocols approved by the Stanford Animal Care and Use Committee.

Note that full information on the approval of the study protocol must also be provided in the manuscript.